Electronic Supplementary Information

Ultra-highly selective trapping of perrhenate/pertechnetate by a flexible cationic coordination framework

Cheng-Peng Li, Jin-Yun Ai, Hang Zhou, Qi Chen, Yijie Yang, Hongming He, and Miao Du*

College of Chemistry, Tianjin Key Laboratory of Structure and Performance for Functional Molecules, MOE Key Laboratory of Inorganic–Organic Hybrid Functional Material Chemistry, Tianjin Normal University, Tianjin 300387, China

* *Corresponding author. E-mail: hxxydm@tjnu.edu.cn*

Chem. Commun.

Experimental details

Materials and general methods. Deionized water was employed throughout the experiments. The tib ligand was purchased from Tianjin Dadikanghe Medical Technology Co. Ltd. Elemental analysis for C, H, and N was performed on a Vario EL III Elementar analyzer. IR spectra were taken on a Bruker Alfa FT-IR spectrometer (with KBr pellet) in 4000–400 cm^{-1}. Powder X-ray diffraction (PXRD) patterns were taken on a Rigaku model Ultima IV diffractometer with Rigaku D/teX ultrahigh-speed position sensitive detector and Cu-Kα X-ray (40 kV and 100 mA), in a step-scan mode with the scan rate of 2 °/min and step size of 0.02°. Simulation of PXRD patterns was carried out using single-crystal diffraction data with the diffraction-crystal module of *Mercury*. Scanning electronic microscopy (SEM) and Energy-dispersive spectroscopy (EDS) were performed on a FEI Nova Nano 230 scanning electron microscope, with the energy of the electron beam being 15 and 20 keV, respectively. Inductively coupled plasma mass spectroscopy (ICP-MS) analysis was conducted by using a Perkin-Elmer ELAN 9000 instrument after degradation of the sample in HNO_3.

Single-crystal X-ray diffraction. Single crystal X-ray diffraction data were collected on an Agilent SuperNova Dual diffractometer with an AtlasS2 detector and Cu Kα radiation (λ = 1.54184 Å) at 100 K for TJNU-216, and 293 K for TJNU-216(Re). Multi-scan absorption corrections were performed using the *SADABS* program. The structures were solved by direct methods, and all non-hydrogen atoms were refined anisotropically by full-matrix least-squares method with the *SHELXTL* crystallographic software package. The final refinement was taken by full-matrix least-squares methods with anisotropic thermal parameters for all non-H atoms on F^2. Generally, C-bound H atoms were geometrically located and refined as riding. Isotropic displacement parameters of H atoms were derived from their parent atoms. $CF_3SO_3^-$ anion in TJNU-216 was treated as the disordered model with 0.52/0.48 occupancies to achieve the appropriate thermal parameters. Further crystallographic data and structural refinement details are shown in Table S1.

Synthesis of TJNU-216

A CH_3CN solution (3 mL) of tib (17.1 mg, 0.05 mmol) was carefully layered onto a water solution (3 mL) of $AgCF_3SO_3$ (19.3 mg, 0.075 mmol) with ethyl acetate as the intermediate layer in a straight glass tube. Colorless block crystals were obtained by slow evaporation of the solvent at room temperature after three days. Yield: 17.3 mg. The crystals were dipped in methanol solution for three days prior to use. Anal. Calcd for $C_{20}H_{15.5}AgF_3N_{8.5}O_3S$: C, 38.76; H, 2.52; N, 19.21%. Found: C, 38.20; H, 2.29; N, 18.65%. IR (cm^{-1}): 1537*s*, 1498*s*, 1260*vs*, 1170*s*, 1110*w*, 1064*s*, 1029*m*, 983*w*, 945*w*, 914*w*, 826*m*, 741*m*, 636*s*, 577*w*, 518*w.*

Synthesis of TJNU-216(Re)

By simply soaking the TJNU-216 crystals (15 mg) into a $KReO_4$ water solution (5 mL, 0.05 mmol) for two days. Good quality crystals were generated and then washed by DMF several times. Anal. Calcd for $C_{21}H_{21}N_9O_5ReAg$: C, 32.61; H, 2.74; N, 16.30%. Found: C, 32.47; H, 2.76; N, 16.22%. IR (cm^{-1}): 1670*s*, 1540*m*, 1495*s*, 1386*w*, 1310*w*, 1244*m*, 1067*s*, 897*vs*, 826*w*, 732*w*, 654*m*.

Anion exchange

As-synthesized TJNU-216 materials (30 mg, 0.05 mmol) were added into the water solution (20 mL) of $KReO_4$ (58 mg, 0.2 mmol) and the mixture was stirred at room temperature. The solids were monitored at various time intervals to follow the exchange progress.

Adsorption kinetics

As-synthesized TJNU-216 materials (15 mg, 0.025 mmol) were immersed into the aqueous solution (10 mL) of $KReO_4$ (72 ppm, 0.25 mM), and stirred at room temperature. Then the solution was separated at different time intervals by a syringe filter (PTFE, 0.25 mm). The anion concentration of ReO_4^- remaining in the water phase and the trapping percentage of ReO_4^- were determined by the ICP-MS measurements.

Adsorption isotherm

As-synthesized TJNU-216 materials (5 mg) were immersed into the water solutions (10 mL)

of $KReO_4$ (1000 ppm, 800 ppm, 500 ppm, 100 ppm, 10 ppm, 1 ppm or 50 ppb, respectively). The mixture was stirred at room temperature for 24 h to make sure that the equilibrium was achieved. The solution was separated from the crystals by a syringe filter (PTFE, 0.25 mm). The anion concentration of ReO_4^- remaining in the water phase and the trapping percentage of ReO_4^- were determined by the ICP-MS measurements. In order to explore the exchange thermodynamics of ReO_4^- by TJNU-216, Langmuir and Freundlich sorption models were applied.

In the Langmuir model, the adsorption of anions was assumed on a homogenous surface of MOF material, following a monolayer adsorption process. No interaction occurs between the anion and the adsorbent, suggesting homogenous binding site and equivalent adsorption energy. The equation of the Langmuir model is

$$\frac{c_e}{q_e} = \frac{1}{q_m k_L} + \frac{c_e}{q_m} \qquad \textbf{(1)}$$

in which c_e is the equilibrium concentration of anion (mg L^{-1}), q_e and q_m are the equilibrium and maximum adsorption amount (mg g^{-1}), and k_L is a constant indirectly related to sorption amount and energy of sorption (L mg^{-1}), characterizing the affinity of the adsorbate with the adsorbent. The fitting line was carried out by plotting c_e/q_e against c_e, and q_m and k_L can be calculated from the slope and intercept.

In the Freundlich adsorption model, it is based on a heterogeneous surface, suggesting different binding energies between the anion and surface sites of MOF. The equation of the Freundlich model is

$$\ln q_e = \ln k_F + \frac{1}{n} \ln c_e \qquad \textbf{(2)}$$

where c_e and q_e are the equilibrium concentration of anion (mg L^{-1}) and equilibrium adsorption amount (mg g^{-1}), and k_F and n are the Freundlich constants which are related to sorption amount (mg g^{-1}) and intensity of adsorption, characterizing the affinity of the adsorbate with the adsorbent.

Hydrolytic stability

As-synthesized TJNU-216 materials (25 mg) were immersed in HNO_3 or NaOH solution of different pH values and stirred at room temperature for 24 h. Then, the solid was collected by filtration and washed with water several times. After that, the solids were used to remove ReO_4^- from the aqueous solutions.

Exchange reversibility

As-synthesized TJNU-216 materials (30 mg, 0.05 mmol) were added into the water solution (20 mL) of $KReO_4$ (58 mg, 0.2 mmol), which was stirred at room temperature for one day. The solids were monitored at various time intervals to follow the exchange progress by ICP-MS. Then, the ReO_4^--loaded TJNU-216 was washed with $NaCF_3SO_3$ solution several times. The solution was separated from solid by a syringe filter (PTFE, 0.25 mm) and the concentration of desorbed ReO_4^- anion in the aqueous phase was determined by the ICP-MS measurement.

Anion selectivity

The effect of SO_4^{2-} was tested by adding TJNU-216 (8 mg) into a water solution (10 mL) containing KReO4 (0.025 mM) and Na_2SO_4 (25 mM, 75 mM, 125 mM, 150 mM, 175 mM, 200 mM, 225 mM, 250 mM, 300 mM, 400 mM or 500 mM). Then, the aqueous solutions after sorption were diluted to proper concentration and the concentrations of ReO_4^- in the dilute solutions were determined by ICP-MS. The competing effect of other anions including NO_3^-, PO_4^{3-}, CH_3COO^-, NO_2^-, and Cl^- were performed by adding TJNU-216 (8 mg) into a water solution (10 ml) containing $KReO_4$ (0.025 mM) containing $NaNO_3$ (7.5 mM), Na_3PO_4 (1.25 mM), $NaNO_2$ (1.25 mM), CH_3COONa (0.5 mM), CH_3SO_3Na (0.5 mM), and NaCl (0.25 mM), respectively. Then, the aqueous solutions after sorption were diluted to proper concentration and the concentrations of ReO_4^- in dilute solutions were determined by ICP-MS.

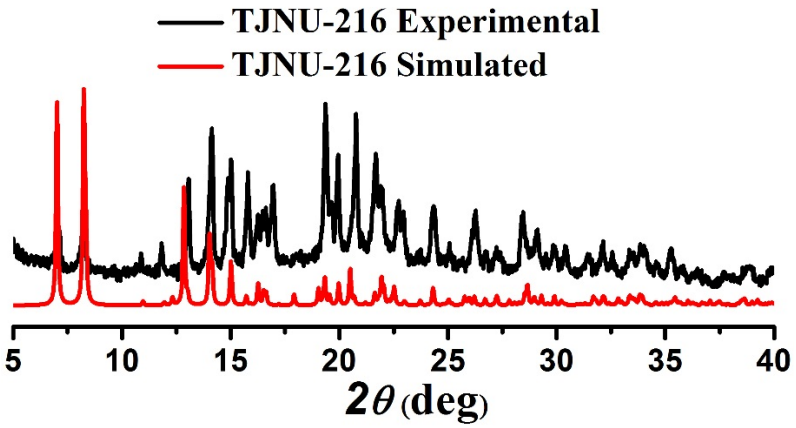

(a)

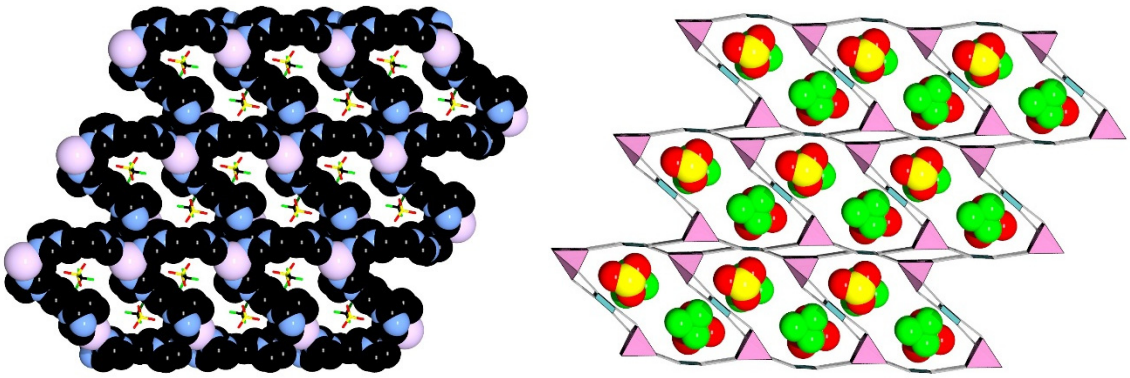

(b) **(c)**

Fig. S1 (a) PXRD patterns of TJNU-216. (b) View of the 3D structure of TJNU-216 along the *a* axis, with the cationic framework showing as space-filling mode. (c) Topological view of the 3D network of TJNU-216. The Ag(I) and tib nodes were simplified as pink tetrahedron and cyan square, respectively.

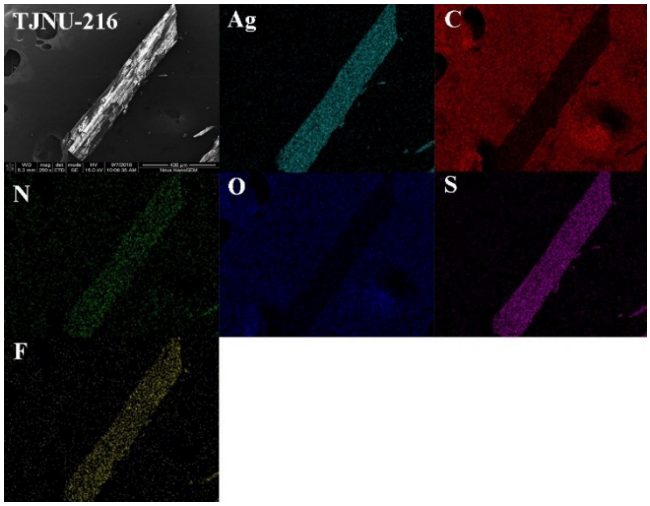

(a)

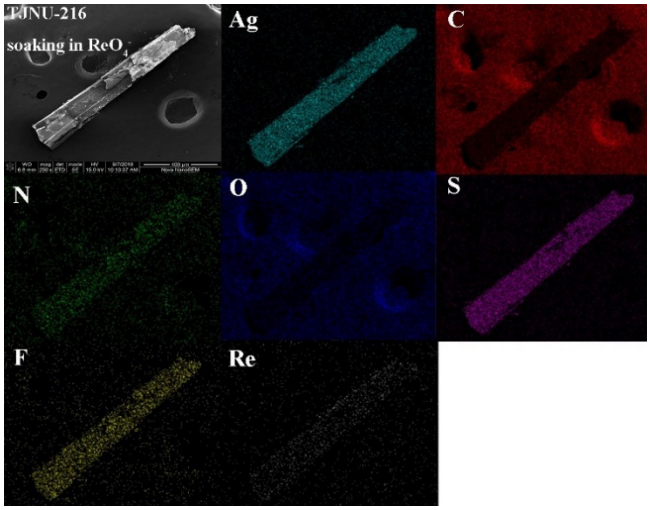

(b)

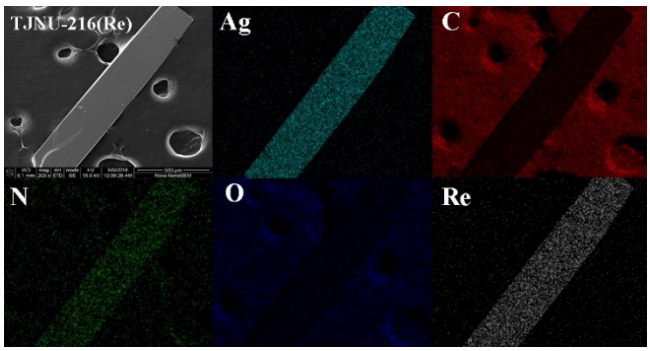

(c)

Fig. S2 SEM images and EDS mapping of TJNU-216 during the anion-exchange process: 0 min (a), 1 min (b), and 10 min (c).

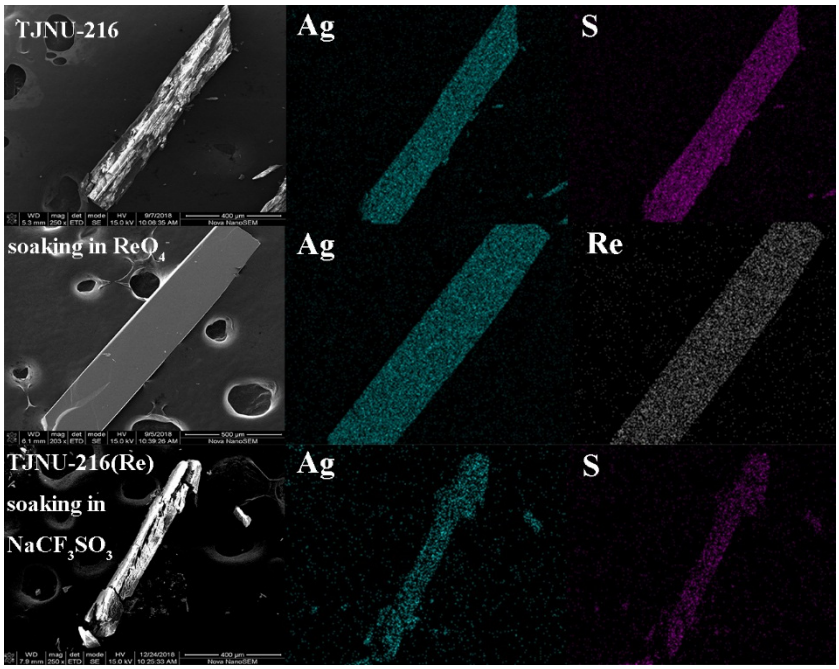

(a)

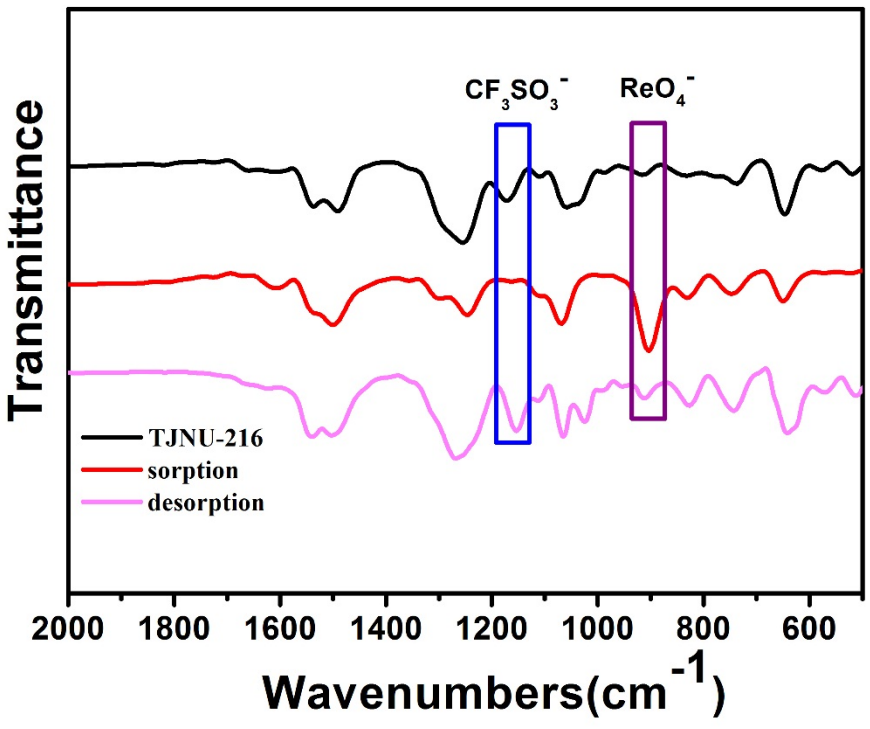

(b)

Fig. S3 SEM-EDS mapping (a) and FT-IR spectra (b) of the TJNU-materials after six cycles.

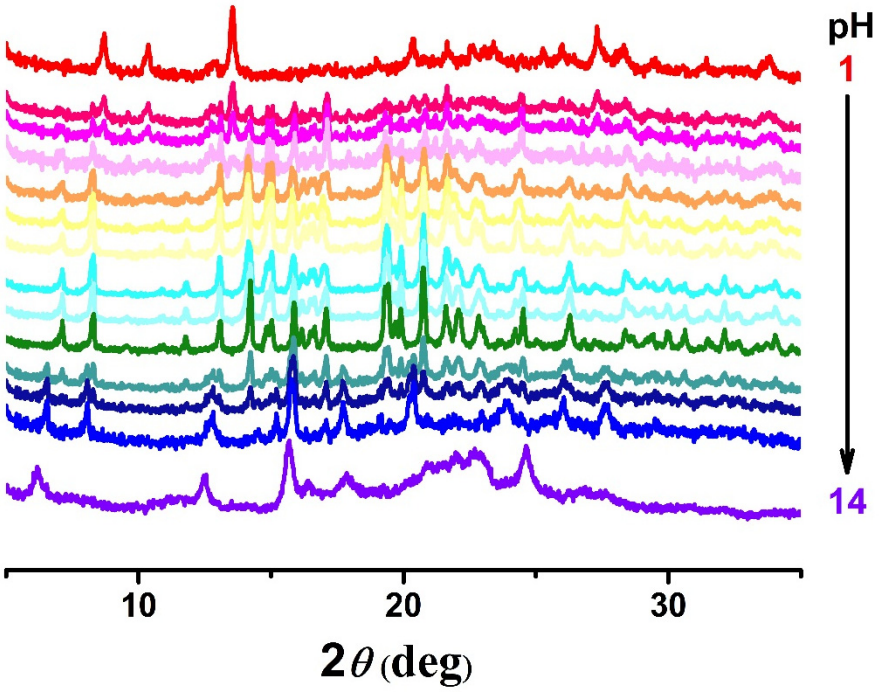

Fig. S4 PXRD patterns of TJNU-216 after immersing in aqueous solutions of pH = 1–14.

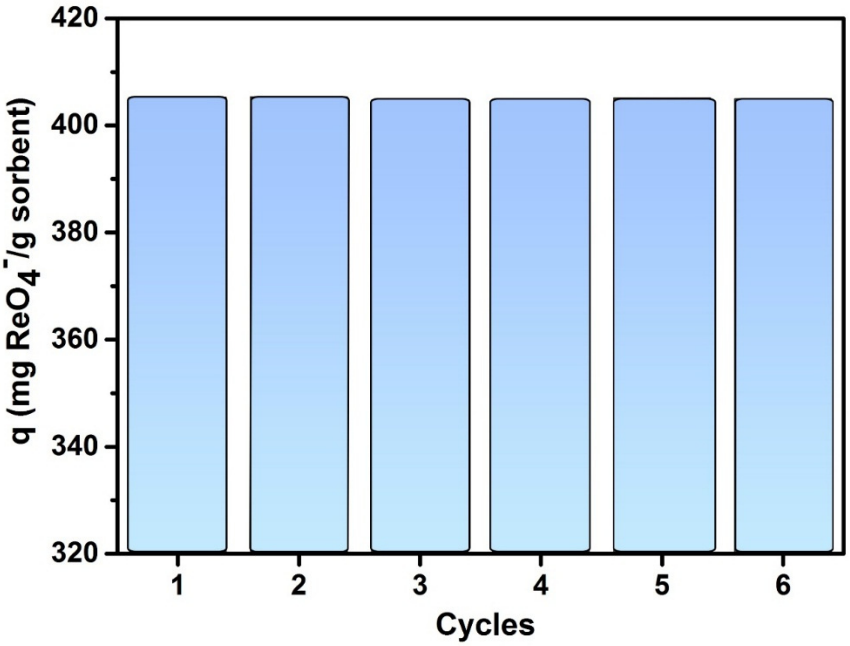

Fig. S5 The uptake capacity of TJNU-216 materials after each cycle.

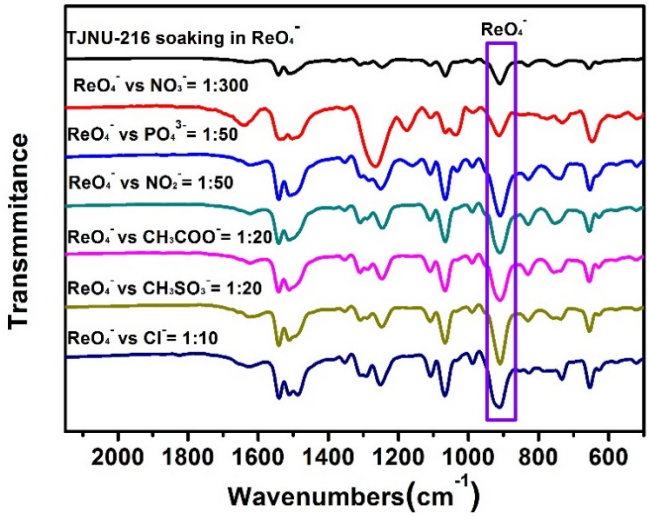

(a)

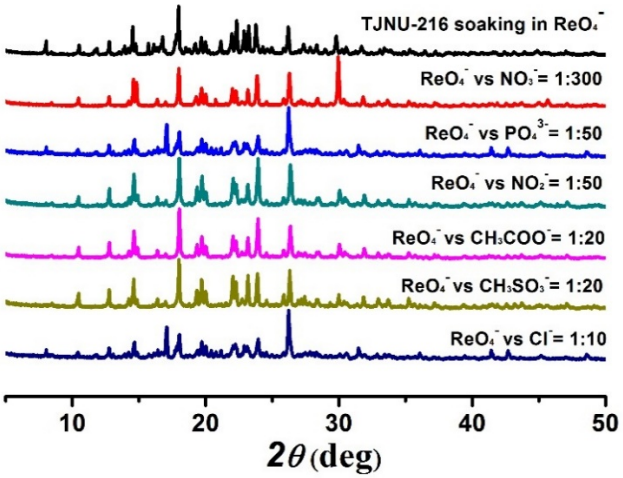

(b)

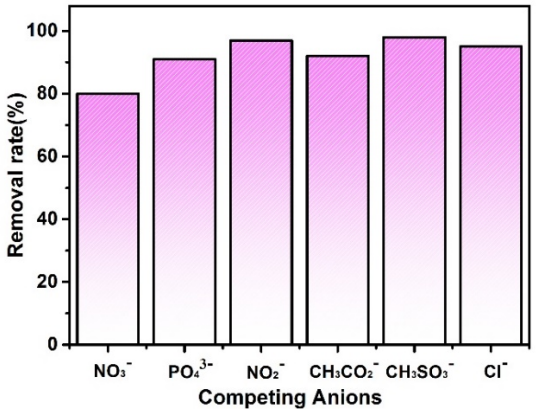

(c)

Fig. S6 FT-IR (a) and PXRD patterns (b) of ReO_4^- loaded TJNU-216. (c) Removal rate of TJNU-216 materials in the presence of ReO_4^- and competing anions with various ratios.

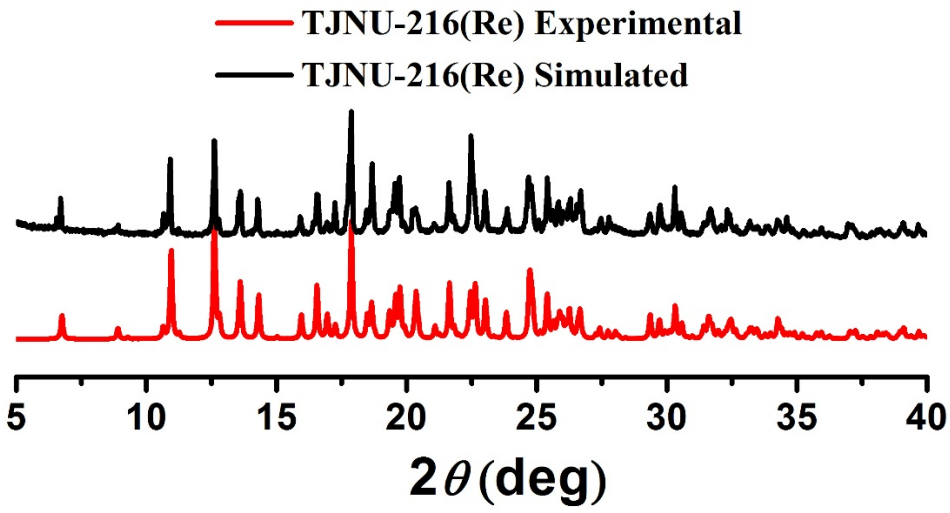

(a)

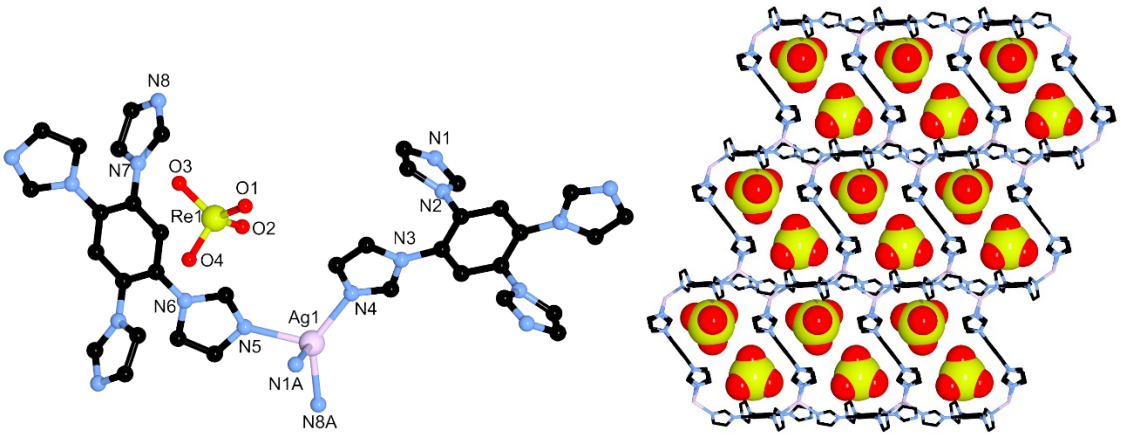

(b) **(c)**

Fig. S7 (a) PXRD patterns of TJNU-216(Re). View of the asymmetric unit (b) and 3D structure (c) of TJNU-216(Re) along the *a* axis, with the ReO_4^- anions showing as space-filling mode.

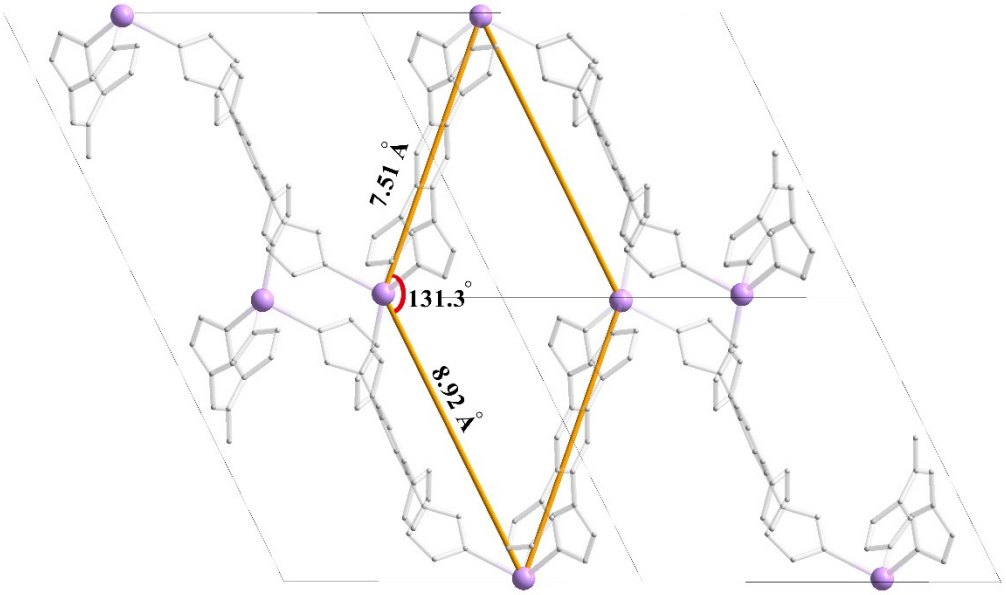

(a)

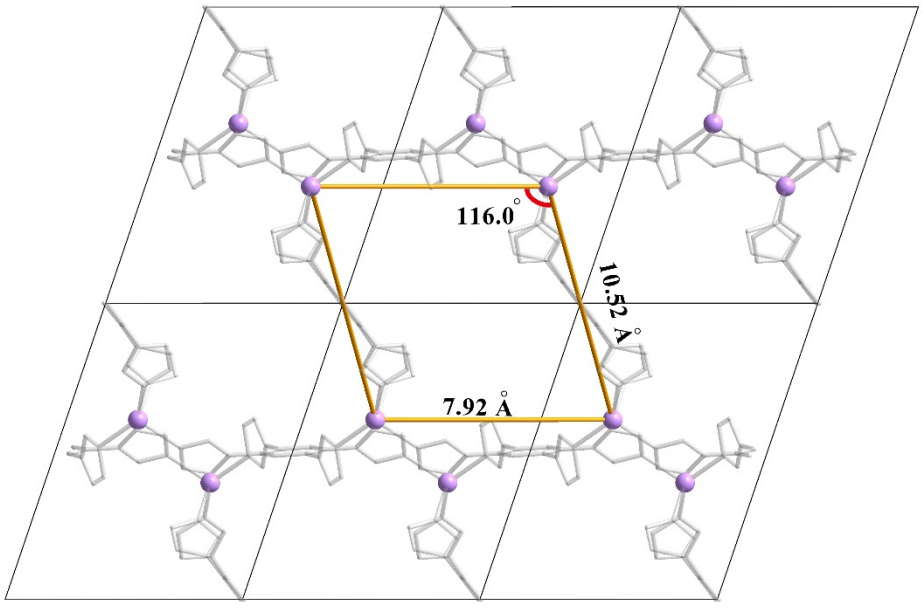

(b)

Fig. S8 The dimensions of the 1D channels in TJNU-216 (a) and TJNU-216(Re) (b).

Table S1 Crystallographic data and refinement details for TJNU-216 and TJNU-216(Re).

	TJNU-216	TJNU-216(Re)
Formula	$C_{20}H_{15.5}AgF_3N_{8.5}O_3S$	$C_{21}H_{21}AgN_9O_5Re$
Formula mass	619.84	773.54
Crystal system	Triclinic	Triclinic
a/Å	8.7133(5)	9.0819(3)
b/Å	12.3600(7)	11.3685(4)
c/Å	13.3642(8)	13.9457(6)
α/°	113.788(6)	103.728(4)
β/°	93.665(5)	98.178(4)
γ/°	107.309(5)	112.943(4)
Unit cell volume/Å^3	1229.18(14)	1242.94(9)
Temperature/K	100.00(10)	293(2)
Space group	*P*-1	*P*-1
Z	2	2
Absorption coefficient, μ/mm^{-1}	0.968	16.152
No. of reflections measured	8892	8212
No. of independent reflections	4327	4857
R_{int}	0.0427	0.0329
Final R_1 values ($I > 2\sigma(I)$)	0.0787	0.0515
Final $wR(F^2)$ values ($I > 2\sigma(I)$)	0.2001	0.1372
Final R_1 values (all data)	0.0955	0.0554
Final $wR(F^2)$ values (all data)	0.2117	0.1419
Goodness of fit on F^2	1.066	1.008

Table S2 Summary on ReO_4^- adsorption efficiency by various anion-exchange materials.

Materials	Adsorption capacity (mg g^{-1})	Removal percent-age (%)	K_d (mL g^{-1})	Ref
PAF-1-F	420	97	2.55×10^4	1
MIL-101(Cr)	215	72	8.9×10^3	1
MIL-101-F	237	87	2.1×10^5	1
SCU-100	541	>99	3.3×10^5	2
SCU-101	217	>95	7.5×10^5	3
UIO-66-NH_3^+	159	66	837	4
SLUG-21	602	95	3.8×10^5	5
Mg-Al-LDH	10	21	262	2
NDTB-1	19	39	652	2
$Y_2(OH)_5Cl$	25	10	112	2
SCU-6	0.06	14	54	6
SCU-7	0.4	90	3×10^3	6
SBN	786	>99	8.3×10^5	7
SCU-CPN-1	999	>99	6.2×10^5	8
TJNU-216	417	>99	8.2×10^5	this work

Table S3 Hydrogen-bonding geometries (Å, °) in the structure of TJNU-216(Re).

D–H···A	$d_{D\cdots A}$	$d_{H\cdots A}$	∠$_{D–H\cdots A}$	Symmetry codes
C8–H8···O2	3.453(13)	2.56	162	
C12–H12···O2	3.191(12)	2.40	142	
C16–H16···O4[a]	3.243(18)	2.42	148	$1-x, -y, 1-z$

Reference

1. D. Banerjee, S. K. Elsaidi, B. Aguila, B. Y. Li, D. Kim, M. J. Schweiger, A. A. Kruger, C. J. Doonan, S. Q. Ma and P. K. Thallapally, *Chem. Eur. J.,* 2016, **22**, 17581.
2. D. Sheng, L. Zhu, C. Xu, C. Xiao, Y. Wang, Y. Wang, L. Chen, J. Diwu, J. Chen, Z. Chai, T. E. Albrecht-Schmitt and S. Wang, *Environ. Sci. Technol.*, 2017, **51**, 3471.
3. L. Zhu, D. Sheng, C. Xu, X. Dai, M. A. Silver, J. Li, P. Li, Y. Wang, Y. Wang, L. Chen, C. Xiao, J. Chen, R. Zhou, C. Zhang, O. K. Farha, Z. Chai, T. E. Albrecht-Schmitt and S. Wang, *J. Am. Chem. Soc.*, 2017, **139**, 14873.
4. D. Banerjee, W. Q. Xu, Z. M. Nie, L. E. V. Johnson, C. Coghlan, M. L. Sushko, D. Kim, M. J. Schweiger, A. A. Kruger, C. J. Doonan and P. K. Thallapally, *Inorg. Chem.*, 2016, **55**, 8241.
5. H. H. Fei, M. R. Bresler and S. R. J. Oliver, *J. Am. Chem. Soc.*, 2011, **133**, 11110.
6. Z. Bai, Y. Wang, Y. Li, W. Liu, L. Chen, D. Sheng, D. Juan, Z. Chai, T. E. Albrecht-Schmitt and S. Wang, *Inorg. Chem.*, 2016, **55**, 6358.
7. L. Zhu, C. Xiao, X. Dai, J. Li, D. Gui, D. Sheng, L. Chen, R. Zhou, Z. Chai, T. E. Albrecht-Schmitt and S. Wang, *Environ. Sci. Technol. Lett.*, 2017, **4**, 316.
8. J. Li, X. Dai, L. Zhu, C. Xu, D. Zhang, M. A. Silver, P. Li, L. Chen, Y. Li, D. Zuo, H. Zhang, C. Xiao, J. Chen, J. Diwu, O. K. Farha, T. E. Albrecht-Schmitt, Z. Chai and S. Wang, *Nat. Commun.*, 2018, **9**, 3007.